

On-line optimization design of sliding mode guidance law with multiple constraints



Q.Z. Zhang^a, Z.B. Wang^a, F. Tao^{a,*}, Bhaba R. Sarker^b

^aSchool of Automation Science and Electrical Engineering, Beihang University, Beijing 100191, China

^bDepartment of Industrial Engineering, Louisiana State University, Baton Rouge, LA 70803-6409, USA

ARTICLE INFO

Article history:

Received 18 April 2012

Received in revised form 4 February 2013

Accepted 21 February 2013

Available online 14 March 2013

Keywords:

Sliding mode guidance

Multiple constraints

Impact angle

SQP

On-line optimization

ABSTRACT

The design of terminal guidance law with impact angle constraint is required for air-to-ground guided weapons to increase their warhead effect. The variable structure guidance law that consists of diving plane guidance and turning plane guidance equations with impact angle constraint is derived, and the saturation function is introduced into the design of reaching law control to weaken the chattering of the guidance system. The influence of four guidance parameters (i.e., reaching law factor, switching item gain, angle error item factor, and boundary layer thickness) on guidance performance is studied and three typical constraints (i.e., heating rate, normal load factor, and dynamic pressure) are analyzed. An optimization model is established for this problem and the feasibility of on-line optimization on guidance law parameters by the Sequential Quadratic Programming (SQP) algorithm is discussed as well. Simulation results show that the on-line optimization of the derived guidance law not only satisfies specified constraints, but also minimizes the fuel cost during the flying course. Moreover, the optimization process can be completed in a few seconds so that it is suitable for on-board applications.

© 2013 Elsevier Inc. All rights reserved.

1. Introduction

A guidance system is a device or a group of devices used to navigate a ship, aircraft, missile, rocket, satellite, or other crafts. It generates guidance laws which take input from the navigation system and use targeting information to send signals to the flight control system that will allow the vehicle to reach its destination.

The main objective of guidance systems for ground striking weapons is to generate suitable commands that produce zero terminal miss-distances. In some cases, however, many kinds of guided weapons are expected not only to get a minimum miss-distance but also to achieve a desired impact angle, so that the warhead of the weapons can acquire better kill effect. A typical example is the design of a ‘homing’ system for certain re-entry vehicles. The terminal attitude angle should be within a permissible range in addition to the miss-distance requirement. Another example is the guidance of air-to-ground weapons with directive warheads. During the final attack, the impact angle should have a preferred value to achieve a proper penetration and ensure high killing probability for some missiles and torpedoes, which attack targets with heavy armors. For the past few decades, a variety of methods for guidance laws with terminal impact angle constraints have been extensively studied. Based on different theories, the existing guidance laws are categorized into *optimal guidance laws*, *proportional navigation guidance laws*, *variable structure guidance laws* and other guidance laws.

* Corresponding author.

E-mail address: ftao@buaa.edu.cn (F. Tao).

Optimal Control Theory (OCT) plays a significant role in the study of impact-angle-constrained terminal guidance. Kim and Grider [1] first derived the optimal and suboptimal guidance laws with constraints on impact angle, which seems to be a pioneering research in this area. Based on this, many studies are started. A planar engagement problem with terminal impact angle constraint was formulated as a numerical optimization problem in Song et al. [2], wherein the angle constraint was treated as a penalty. Ryoo et al. [3] investigated the closed-form solutions of optimal guidance laws and expressed the entire missile states using polynomial functions in terms of time-to-go. At the same time, a generalized formulation of energy minimization optimal guidance law for constant speed missiles was proposed in Lee et al. [4] to control impact angle, terminal acceleration and miss-distance. Ryoo et al. [5] presented the optimal guidance laws for arbitrary missile dynamics and derived the specific forms of the state feedback for lag-free and first-order lag systems. Based on this, a new optimal guidance law for constant speed missiles was proposed in Ryoo et al. [6] by including a time-varying weighing function in the cost of control energy to improve the performance of the guidance system against external disturbances or sensor measurement noises. For further the research of Lee et al. [4], a suboptimal guidance with the terminal constraints on impact angle, acceleration, and time-derivative of acceleration was presented in Lee et al. [7], wherein the control input consists of an additional feed-forward command and an optimal feedback command. In Subchan [8], the problem of air-to-ground missile guidance with impact angle constraint was reinterpreted using OCT and transformed into a minimum integrated altitude problem, which was solved by an indirect method. Different from this, a three-dimensional guidance law with impact angle constraint was proposed by Ma et al. [9] using Lyapunov stability theory. Kim et al. [10] further dealt with the guidance and control system to impact a target with a desired impact angle for precision guided bombs and derived the control based on the solution of the linear quadratic optimal control problem. Then a nonlinear suboptimal guidance law was synthesized in Oza and Padhi [11,12] using recently developed Model Predictive Static Programming (MPSP) for successful interception of ground targets. The main feature of this guidance law is that it accurately satisfies terminal impact angle constraints in both azimuth and elevation, simultaneously. As a new trial, Xing and Chen [13] considered the constraints on both terminal flight path angle and terminal angle of attack, and derived the guidance law by solving the linear quadratic terminal control problem. More recently, the analytic solutions of the generalized and optimal impact-angle-control guidance laws for a first-order lag system were investigated in Lee et al. [14,15], respectively, to examine the effects of system lag on performance of the guidance laws. Furthermore, the work presented in [16] illustrated the optimality of linear time-varying guidance laws for controlling impact angles as well as terminal miss-distances using the inverse problem of OCT.

Proportional Navigation is another approach adopted by many researchers in the design of terminal impact-angle-constrained guidance laws except for OCT. It is well known that the standard Proportional Navigation Guidance (PNG) law cannot achieve an acceptable performance in terms of the impact angle. It is necessary to find new ways to take the terminal angular constraint into consideration in the deviation of the terminal PNG laws. The guidance method discussed in Kim et al. [17] added a time-varying bias term in the conventional PNG to achieve the final impact angle condition, which made assumptions of constant velocity and small error angles. Then a variable structure proportional navigation law for the passive homing missile was designed by Song and Zhang [18] to hit the target with a minimum miss-distance and desired impact attitude angle within the required overload. Besides, a kind of Biased Proportional Navigation Guidance (BPNG) to get an arbitrary impact angle against stationary target was proposed in Jeong et al. [19] and the closed form solution of this guidance was derived. Furthermore, an adaptive proportional guidance law with terminal angular constraint was derived in Hu and Cai [20] for the ground stationary target and an adaptive guidance parameter updating method was presented. In addition, proportional navigation based guidance laws for impact angle constrained interception of moving and stationary targets were studied in Ratnoo and Ghose [21–23]. Similar as these research, Erer and Merttopcuoglu [24,25] devised a method to control the impact angle in an indirect manner by employing biased Pure Proportional Navigation (PPN) as the guidance law, and then the impact angle value against a stationary target became a function of both initial angular conditions and integral of the bias value. Moreover, a guidance law that is capable of achieving a wide range of impact angles was designed in Akhil and Ghose [26] based on the BPNG, which used small angle approximations to derive the bias term for impact angle requirement.

In the past few decades, *Variable Structure Control* (VSC) and associated *Sliding Mode Control* (SMC) have been developed and applied enormously. Considering their good performance on controlling nonlinear plants, the VSC and SMC technologies have been introduced into the design of guidance laws to improve their robustness. In early 1990, the VSC theory was applied to guidance law design of air-to-air missile by Brierley and Longchamp [27], following which numerous guidance laws emerged based on different background. A homing guidance with terminal angular constraint was stated in Kim et al. [28] by employing a Lyapunov-like function with the SMC methodology, but the problem is how to choose suitable guidance parameters. Then a new guidance method called optimal sliding mode guidance law, which integrates optimal guidance with sliding mode guidance was derived by Zhou et al. [29] to achieve robustness against target maneuver. And then an adaptive reaching law of the sliding mode was presented and used to derive an adaptive sliding mode guidance law by Zhou et al. [30]. Based on these studies, a scheme of integrated guidance/autopilot design for missiles with impact angle constraints was studies in Xu et al. [31] based on the back-stepping idea and VSC theory. And a new three-dimensional variable structure guidance law was discussed in Sun and Zheng [32] based on adaptive model-following control. For further understanding and the research of guidance laws, Hu et al. [33] derived a kind of variable structure guidance law with terminal angular constraint and discussed the feasibility of off-line optimization on guidance law parameters by genetic algorithm, and tested the effect of guidance parameters under the conditions of different initial state bias. However, from the simulation results, the optimization process costs so much time that the guidance law unfits for the on-line application. For more complicated

situations, a new integrated guidance and control design scheme based on VSC approach for missile with terminal impact angle constraint was proposed in Wu and Yang [34], wherein nonlinear transformation was employed to transform the mathematical model into a standard form suitable for SMC method design. Meanwhile, Gu et al. [35] presented a variable structure guidance law with constraint on impact angle that can be implemented conveniently with little target information. And the disturbances such as the estimation errors, the target's velocity, and the target's maneuver acceleration can be successfully restrained by choosing appropriate guidance parameters. For further research, a new scheme of integrated guidance and autopilot design was proposed in Guo and Zhou [36] by adopting the SMC for the case of homing missile against ground fixed target with impact angular constraint. And the same problem was solved using H_∞ control method in Guo and Zhou [37]. Based on the finite time convergence stability theory and the VSC, a finite time convergent sliding mode guidance law with terminal impact angle constraint was presented in Zhang et al. [38]. At the same time, a 3-dimensional robust guidance law was developed for impact angle control in Hu et al. [39] by combining the linear quadratic optimal theory with the VSC methodology. Recently, an approach to impact time and angle guidance was presented in Harl and Balakrishnan [40] through a combination of a novel line-of-sight (LOS) rate shaping technique and a new second-order sliding mode approach. Then, a kind of SMC-based guidance law was proposed in Kumar et al. [41,42] to intercept stationary, constant velocity, and maneuvering targets at a desired impact angle, which was defined in terms of a desired LOS angle. In addition, an autopilot was designed in Kumar et al. [42] as a dynamic sliding-mode controller that enables the tracking of the command generated by the guidance laws. The guidance laws could intercept the targets at any impact angle even in the presence of large initial heading errors, so the so-called "all-aspect interceptor" could be achieved.

Except for the approaches introduced above to the problem of impact angle control for terminal guidance, there are many other studies focusing on the same problem based on different methods. Manchester and Savkin [43] presented a precision guidance law named "Circular Navigation Guidance" (CNG) with impact angle constraint for a two-dimensional planar intercept based on the principle of following a circular arc to the target. As and different trial, the impact angle control problem was formulated as an infinite horizon non-linear regulator problem and solved by the State-Dependent Riccati Equation (SDRE) technique in Ratnoo and Ghose [44,45]. Similar study based on modifying SDRE technique was carried out by Bardhan and Ghose [46]. Considering the performance limit of the Separated Guidance and Control (SGC) loop, a concept of the Integrated Guidance and Control (IGC) was introduced in Yun and Ryoo [47] and a new type of IGC with impact angle constraint was derived using the Linear Quadratic Regulator (LQR). Besides, a cubic spline guidance law was obtained from cubic-spline-curve-based trajectory using an inverse method in Dhabale and Ghose [48] for intercepting a stationary target at a desired impact angle. The cubic spline trajectory curve expressed the altitude as a cubic polynomial of the downrange. Then, a new three-dimensional guidance law with high impact angle constraints used for striking ground moving targets was designed in Zhang et al. [49] based on back-stepping control approach. To ensure the required impact angle and small miss-distance, two step controllers were designed based on Lyspunov method. Aiming at the shortage of CLC (circular arc-straight line-circular arc) path planning, CCC (three circular arcs) path planning was adopted to control impact time and impact angle in Zhang et al. [50]. The latest research in this area can be found in Lee et al. [51], which proposed the impact angle control guidance laws with terminal acceleration constraints for a stationary or slowly moving target. These laws are called Time-to-go Polynomial Guidance (TPG) which assumes the guidance command as a polynomial function of time-to-go and determines the coefficients of the guidance command to satisfy the specified terminal constraints.

As can be seen from the optimal guidance laws, the guidance problems with terminal angular constraints are transformed into optimal control problems with terminal constraint conditions, and then forms the optimal guidance laws based on the OCT, which could minimize the velocity lost, the flying time, or the fuel cost. According to the deviation of terminal PNGs, one or more terms are added in the expression of the guidance laws to satisfy the terminal angular constraints. Besides, the desired impact angle constraint can also be included into the sliding mode to form the sliding mode guidance laws in more robust ways. All of these guidance laws are designed not only to get a minimum miss-distance but also to achieve a desired impact attitude angle to acquire better kill effect; however, the complex environment the vehicles will experience and the requirements of fuel cost during the flying course are neglected. Actually, the guided weapons will face up to harsh conditions and typical constraints brought by dense atmosphere during the striking, for example, the heating rate, normal load factor and dynamic pressure. However, these severe conditions have not been considered in former studies. Though the off-line optimization on guidance law parameters by genetic algorithm is studied in Hu et al. [33], the whole searching process casts too much time to be applied on-line. So the main concern of this paper is the multi-constraints-based optimization of terminal guidance law with its on-line application.

In detail, the primary works and contribution of this paper can be concluded as follows:

1. A quasi-sliding mode guidance law is design using boundary layer method for terminal impact-angle-constrained engagement with stationary target and the influence of guidance parameters (i.e., reaching law factor, switching item gain, angle error item factor, and boundary layer thickness) on the guidance performance is analyzed.
2. In addition to the requirement of impact angle constraint, we further consider several hard constraints (i.e., heating rate, normal load factor and dynamic pressure) and control constraints (i.e., maximum angle of attack and sideslip angle) during the striking. Then the optimization model is established to minimize the integrated performance index consisting of the fuel expenditure and velocity lost.

3. In order to achieve the on-line optimization design of the terminal sliding mode guidance law, we implement a fast convergence Sequential Quadratic Programming (SQP) algorithm to solve the established optimization problem. Simulation results show that the whole optimization process can be completed in a few seconds, which promotes the on-line application of this approach.

The rest of this paper is organized as follows. Section 2 establishes the equations of motion for the weapon-target engagement. A terminal guidance law based on the SMC methodology is designed in Section 3 to eliminate the miss-distance and achieve a desired impact angle. Then the influence of each guidance law parameter on the guidance performance is discussed in Section 4. In order to achieve the on-line optimization and application of the guidance law, the optimization model based on SQP algorithm is established in Section 5. Simulation studies are carried out in Section 6 to investigate the feasibility of the SQP algorithm for the on-line optimization of the guidance parameters. Finally, conclusions and possible future work are discussed in Section 7.

2. Equations of motion

In order to simplify the equations of the striking situation, the weapon-target engagement model is divided into diving plane and turning plane as shown in Fig. 1 (see [52]). An earth-fixed coordinate system is defined. The target is stationary and stays at the origin of the coordinate system. The y -axis is pointed to the up and deviates from the Earth center, the x -axis stays in the horizontal plane and is pointed to the weapon, and the z -axis completes the right-hand system. It is also assumed that the angle of attack is small and its velocity is constant.

The standard three-dimensional equations of motion of the guided weapon over a flat earth can be represented by the following nonlinear differential equations (see [52]).

$$\begin{cases} \dot{v} = (R_{xh} + P_{xh})/m + g_{xh}, \\ \dot{\theta} = (R_{yh} + P_{yh})/(mv) + g_{yh}/v, \\ \dot{\sigma} = -(R_{zh} + P_{zh})/(mv \cos \theta) - g_{zh}/(v \cos \theta), \\ \dot{x} = v \cos \theta \cos \sigma, \\ \dot{y} = v \sin \theta, \\ \dot{z} = -v \cos \theta \sin \sigma, \end{cases} \quad (1)$$

where $\dot{x}, \dot{y}, \dot{z}$ are the change rate of position coordinates x, y, z , respectively. v is the earth relative velocity and \dot{v} denotes the acceleration. The flight path angle and angular rate are θ and $\dot{\theta}$, while the velocity deflection angle and angular rate are σ and $\dot{\sigma}$. R_{xh}, R_{yh} and R_{zh} are the aerodynamic force decomposition described in velocity coordinate system as g_{xh}, g_{yh}, g_{zh} and P_{xh}, P_{yh}, P_{zh} represent the gravity acceleration decomposition and propulsion decomposition, respectively. The mass m is a constant.

As shown in Fig. 1, the motion of weapon can be decomposed in diving plane and turning plane. The LOS ρ from the target to the weapon is defined by elevation angle λ_D and azimuth angle λ_T . v_D and v_T are the velocity decomposition respectively in diving plane and turning plane. λ_{TT} is the azimuth angle in the turning plane. The equation of weapon-target relative movement can be found in Zhao [52]

$$\begin{cases} \ddot{\lambda}_D = (\dot{v}/v - 2\dot{\rho}/\rho)\dot{\lambda}_D - \dot{\rho}\dot{\gamma}_D/\rho, \\ \ddot{\lambda}_{TT} = (\dot{v}/v - 2\dot{\rho}/\rho)\dot{\lambda}_{TT} + \dot{\rho}\dot{\gamma}_T/\rho, \end{cases} \quad (2)$$

where γ_D and γ_T denote the azimuth angle of velocity in diving plane and turning plane respectively, and their angular rate are $\dot{\gamma}_D$ and $\dot{\gamma}_T$. $\dot{\rho}$ is the change rate of LOS. $\dot{\lambda}_D$ and $\ddot{\lambda}_D$ are the angular rate and angular acceleration of elevation angle λ_D , $\dot{\lambda}_{TT}$ and $\ddot{\lambda}_{TT}$ denote the angular rate and angular acceleration of azimuth angle in the turning plane λ_{TT} .

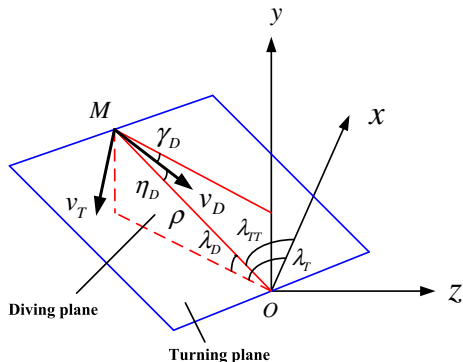


Fig. 1. Coordinate system and geometry.

3. Variable structure guidance law derivation

Due to the inherent robustness and relatively simple control algorithm of the sliding mode VSC system, the VSC theory is gradually applied to the design of guidance laws. Most of the current researches on variable structure guidance laws are confined to two-dimensional plane, and how to select the guidance parameters also lack a conclusion. Because the sliding mode can be designed according to need and is independent of parameters and disturbances of the object, the desired impact attitude can be included into the sliding mode and derive the variable structure guidance laws with terminal angular constraint, which performs strong robustness on uncertainty factors. Next we will design the guidance laws in diving plane and turning plane, respectively, and then introduce the Quasi-Sliding Mode Variable Structure Control (QSMVSC) theory to reduce the chattering brought by switching.

3.1. Diving plane guidance equation

In order to apply the SMC methodology to the guidance problem, a switching surface is to be chosen first. In the guidance problem with terminal angular constraint, the guidance goal is transformed into achieving zero miss-distance and a desired impact attitude angle, simultaneously. So the switching surface should include these two factors. The miss-distance condition is represented by LOS rate $\dot{\lambda}_D = 0$, and the terminal impact attitude angular constraint is satisfied by nulling LOS error $|\lambda_D + \gamma_{DF}|$. So the switching surface of this section is chosen such that

$$S_1 = \dot{\lambda}_D + \lambda_1 v \cdot (\lambda_D + \gamma_{DF})/\rho, \quad (3)$$

where the angle error item factor λ_1 is a positive constant. The first term is responsible for the miss-distance and the second term is responsible for the impact attitude angle. γ_{DF} denotes the desired impact angle, which is a constant since the target is fixed.

A sufficient condition in order to guarantee the attractiveness of sliding mode $S_1 = 0$ is $S_1 \cdot \dot{S}_1 < 0$. The reaching law is chosen as

$$\dot{S}_1 = -k_1/T_g \cdot S_1 - \varepsilon_1/\rho \cdot \text{sgn}(S_1), \quad (4)$$

where the reaching law factor k_1 and the switching item gain ε_1 are both positive constants. T_g is the time-to-go and sgn denotes the sign function.

Differentiating Eq. (3) with respect to t and combined with Eq. (1), the following holds.

$$\dot{S}_1 = (\dot{v}/v - 2\dot{p}/\rho)\dot{\lambda}_D - \dot{p}\dot{\gamma}_D/\rho + \lambda_1 \dot{v}(\lambda_D + \gamma_{DF})/\rho + \lambda_1 v \dot{\lambda}_D/\rho - \lambda_1 v \dot{p}(\lambda_D + \gamma_{DF})/\rho^2. \quad (5)$$

Comparing Eq. (4) with Eq. (5), and considering $T_g = -\rho/\dot{p}$, the diving plane guidance equation can be obtained.

$$\dot{\gamma}_D = -T_g \{(\dot{v}/v + (k_1 + 2)/T_g + \lambda_1 v/\rho)\dot{\lambda}_D + [\lambda_1 \dot{v}/\rho + \lambda_1 v(k_1 + 1)/(\rho T_g)] \cdot (\lambda_D + \gamma_{DF}) + \varepsilon_1/\rho \cdot \text{sgn}(S_1)\}. \quad (6)$$

3.2. Turning plane guidance equation

In the turning plane, we only consider the condition $\dot{\lambda}_{TT}(t_f) = 0$ at final time t_f . Similarly, the switching surface is chosen as $S_2 = \dot{\lambda}_{TT}$ and the reaching law is chosen as $\dot{S}_2 = -k_2/T_g \cdot S_2 - \varepsilon_2/\rho \cdot \text{sgn}(S_2)$. Considering $\dot{\lambda}_{TT} = \dot{\lambda}_T \cos \lambda_D$, the turning plane guidance equation can also be easily obtained.

$$\dot{\gamma}_T = T_g \{[\dot{v}/v + (k_2 + 2)/T_g]\dot{\lambda}_T \cos \lambda_D + \varepsilon_2/\rho \cdot \text{sgn}(S_2)\}. \quad (7)$$

3.3. Guidance law with quasi-sliding mode control

The variable structure guidance law performs good stability at the expense of high frequency chattering, which can reduce the precision of the control system, increase the fuel cost and destroy the performance of the system. This problem can be solved by replacing the sign function with the saturation function (see [53])

$$\text{sat}(S) = \begin{cases} 1 & S > \Delta, \\ S/\Delta & |S| \leq \Delta, \\ -1 & S < -\Delta, \end{cases} \quad (8)$$

where the thickness of boundary layer Δ is a positive constant. Then, expressions (6) and (7) become (see [33])

$$\begin{cases} \dot{\gamma}_D = -T_g \{(\dot{v}/v + (k_1 + 2)/T_g + \lambda_1 v/\rho)\dot{\lambda}_D + [\lambda_1 \dot{v}/\rho + \lambda_1 v(k_1 + 1)/(\rho T_g)] \cdot (\lambda_D + \gamma_{DF}) + \varepsilon_1/\rho \cdot \text{sat}(S_1)\}, \\ \dot{\gamma}_T = T_g \{[\dot{v}/v + (k_2 + 2)/T_g]\dot{\lambda}_T \cos \lambda_D + \varepsilon_2/\rho \cdot \text{sat}(S_2)\}, \end{cases} \quad (9)$$

where k , λ , ε and Δ with subscripts 1 and 2 denote guidance parameters of diving and turning plane, respectively. This is the terminal guidance law based on QSMVSC methodology to minimize the miss-distance and satisfy the impact angle constraint. This guidance law can weaken the chattering brought by switching and is not sensitive to external disturbances.

4. Influence of guidance parameters

The variable structure guidance law includes four guidance parameters: k , ε , λ and Δ . It is necessary to analyze the influence of the four parameters on the guidance performance before the optimization. It is known that the movement of ground striking weapon is mainly in the diving plane and the side guidance has less impact on the precision of miss-distance and terminal attitude angle, so only discussing the influence of k_1 , λ_1 , ε_1 and Δ_1 is acceptable.

In order to analyze the influence of the four parameters and investigate the properties of the guidance law for impact angle control, three-dimensional nonlinear simulations with the initial conditions shown in Table 1 are performed. The desired impact angle is chosen as $\gamma_{DF} = -90^\circ$.

4.1. Reaching law factor, k_1

From Eq. (4), we can see that the factor k_1 influences the reaching rate of the sliding mode. Then we chose ε_1 , λ_1 , Δ_1 as the standard values $\varepsilon_1 = 1$, $\lambda_1 = 1$, $\Delta_1 = 0.001$, and discuss the effect of the reaching law factor k_1 on the guidance performance. Table 2 shows the simulation results.

From Table 2, we can find that the terminal velocity, angle of attack, impact angle error and the Circular Error Probable (CEP) change very small with different k_1 s; but the performance index J , which represents the fuel expenditure and velocity lost, decreases with increasing k_1 . The performance index J is defined by

$$J = \frac{1}{2} \int_0^{t_f} (C_1 n_y^2 + C_2 \alpha^2) dt, \quad (10)$$

where n_y is the non-dimensional normal load factor in g and α is the angle of attack in deg. C_1 and C_2 are the weighting coefficients that are assumed to be 1 and 10, respectively.

4.2. Switching item gain, ε_1

From Eq. (4), we can find that the gain ε_1 also affects the reaching rate of the sliding mode. Then we chose k_1 , λ_1 , Δ_1 as $k_1 = 1$, $\lambda_1 = 1$, $\Delta_1 = 0.001$, and analyze the impact of the switching item gain ε_1 on the guidance performance. The simulation results are as shown in Table 3.

Table 3 shows that the three trajectories are basically coincident and the terminal parameters also behave tiny changes with changing ε_1 ; however, with increasing ε_1 , the performance index J diminishes, and the magnitude of normal load factor and angle of attack change intensely.

4.3. Angle error item factor, λ_1

Eq. (3) indicates that the factor λ_1 determines the weight of angle error item in switching function S. Choosing k_1 , ε_1 , Δ_1 as the standard values $k_1 = 1$, $\varepsilon_1 = 1$, $\Delta_1 = 0.001$, and discussing the influence of angle error item factor λ_1 on the guidance performance. The simulation results are reported in Table 4.

It is evident from Table 4 that with increasing λ_1 , the CEP and terminal angle of attack change a little, and the impact angle error and terminal velocity keep nearly invariable. The numerical value of performance index J varies enormously. So the factor λ_1 plays a more important role in guidance performance compared with k_1 and ε_1 .

4.4 Boundary layer thickness, Δ_1

According to the quasi-sliding mode control theory, the thickness of boundary layer Δ_1 has an influence on chattering and guidance performance. Similarly, we chose k_1 and λ_1 as the standard values, and $\varepsilon_1 = 10$. Then analyze the impact of the boundary layer thickness Δ_1 on the guidance performance. The simulation results are as follows.

Table 1
Numerical values for simulation.

Initial position (x_0, y_0, z_0)	(10, 16, -10) km
Initial velocity (v_0)	340 m/s
Initial heading angle (θ_0)	0°
Initial deflection angle(σ_0)	-120°

Table 2Comparisons of the effects for different k_1 s ($\gamma_{DF} = -90^\circ$).

k_1	CEP (m)	θ_f (°)	α_f (°)	v_f (m/s)	J
0.1	0.0798	-90.1565	-0.1750	677.2032	749.3447
1.0	0.2097	-89.9250	-0.1725	681.0937	746.5281
10.0	0.6126	-89.2406	-0.0388	680.5330	737.7190

Table 3Comparisons of the effects for different ε_1 s ($\gamma_{DF} = -90^\circ$).

ε_1	CEP (m)	θ_f (°)	α_f (°)	v_f (m/s)	J
0.1	0.0441	-90.1663	-0.1769	677.2492	750.3775
1.0	0.2097	-89.9250	-0.1725	681.0937	746.5281
10.0	0.1883	-89.9750	-0.1791	680.3869	737.9296

Table 4Comparisons of the effects for different λ_1 s ($\gamma_{DF} = -90^\circ$).

λ_1	CEP (m)	θ_f (°)	α_f (°)	v_f (m/s)	J
0.1	0.9037	-89.4823	-0.2938	676.5685	707.2557
1.0	0.2097	-89.9250	-0.1725	681.0937	746.5281
10.0	0.0446	-90.0260	-0.0081	681.1353	1201.5332

Table 5Comparisons of the effects for different Δ_1 s ($\gamma_{DF} = -90^\circ$).

Δ_1	CEP (m)	θ_f (°)	α_f (°)	v_f (m/s)	J
0.0001	0.8566	-89.5853	-0.1103	680.0898	762.3297
0.001	0.1883	-89.9750	-0.1791	680.3869	737.9296
0.01	0.3083	-90.2705	-0.1864	681.0053	745.1327

Table 5 shows that, the guiding precision and controlling performance change very small with different Δ_1 s, but undersize Δ_1 can cause severe chattering, which can reduce the precision of the guidance system.

In general, the selection of guidance parameters should guarantee the high guiding precision first. To achieve better striking effect and avoid the saturated command, minimizing the miss-distance and terminal normal load factor is required. In addition, the fuel cost and the constraints of heating rate, normal load factor and dynamic pressure should also be considered. So the parameters of variable structure guidance law should be designed and optimized under above considerations.

5. On-line optimization of guidance law with SQP algorithm

The feasibility of off-line optimization on guidance law parameters by genetic algorithm is discussed in Hu et al. [33]; but it costs so much time and limits the on-board application of the guidance law. In order to accomplish the goal of on-line application for the ground striking weapon, it is necessary for us to redesign the optimal guidance law parameters under multiple constraints with other efficient optimization methods.

Many optimization problems in aeronautics and astronautics can be formulated as optimal control problems. Stryk and Bulirsch [54] gives a brief list of commonly used direct and indirect efficient methods for the numerical solution of these problems. For some special weakly nonlinear low dimensional systems the solution can be derived analytically from the sufficient and necessary conditions of optimality; but to obtain a solution of dynamic systems described by strongly nonlinear differential equations, it is necessary to use numerical methods.

Stochastic approaches such as Genetic Algorithm (GA), Particle Swarm Optimization (PSO) and Simulated Annealing (SA) algorithms are used for many kinds of optimization problems (see [55–58]). Many other methods are also proposed to improve the optimization performance (see [59,60,56,57]). In recent years, general-purpose SQP methods have been considerably developed and applied to trajectory optimization and other optimization problems with linear and nonlinear constraints (see [61–64]). Some practical and theoretical aspects of applying SQP methods to optimal control problems are discussed in [65]. These methods can be shown to converge to a solution under very mild conditions on the problem. Terminal guidance law on-line optimization problem is a typical nonlinearly constrained optimization problem, which can be solved by SQP methods.

The performance index is defined by Eq. (10) which represents the fuel expenditure and the velocity lost during the striking course. At the same time, the guidance law parameters should also be selected to satisfy the typical constraints such as

heating rate, normal load factor and dynamic pressure constraints, and maximum angle of attack and sideslip angle constraints. So our goal is to search for adaptable guidance law parameters which not only satisfy the specified constraints but also minimize the performance index.

Here we divide the total time interval $[0, t_f]$ into $n - 1$ equal subintervals of length h each by the points $\{t_1, t_2, \dots, t_n\}$ with $t_1 = 0$ and $t_n = t_f$. Then minimizing the performance index is equivalent to minimizing

$$J^* = \frac{1}{2} \cdot \sum_{i=1}^{n-1} (C_1 n_{yi}^2 + C_2 \alpha_i^2) \cdot h. \quad (11)$$

When the step size h is fixed, it is appropriate to minimize the numerical value of $(C_1 n_{yi}^2 + C_2 \alpha_i^2)$ relates to the real-time guidance law parameters in each interval instead of (11).

In each interval $[t_i, t_{i+1}]$, $i = 1, 2, \dots, n - 1$, when given the vector of state variables $\mathbf{X}_i = (v_i, \theta_i, \sigma_i, x_i, y_i, z_i)$, the current guidance law can be derived.

$$\begin{cases} \dot{\lambda}_D = -T_g \left\{ (\dot{v}_{i-1}/v_i + (k_1 + 2)/T_g + \lambda_1 v_i/\rho) \dot{\lambda}_D + [\lambda_1 \dot{v}_{i-1}/\rho + \lambda_1 v_i(k_1 + 1)/(\rho T_g)] \cdot (\lambda_D + \gamma_{DF}) + \varepsilon_1/\rho \cdot \text{sat}(S_{1i}) \right\}, \\ \dot{\lambda}_T = T_g \left\{ [\dot{v}_{i-1}/v_i + (k_2 + 2)/T_g] \dot{\lambda}_T \cos \lambda_D + \varepsilon_2/\rho \cdot \text{sat}(S_{2i}) \right\}, \end{cases} \quad (12)$$

where \dot{v}_{i-1} is the velocity rate of last step, and

$$\begin{cases} \lambda_D = \arctan(y_i/\sqrt{x_i^2 + z_i^2}), \\ \lambda_T = \arctan(-z_i/x_i), \end{cases}$$

$$\begin{cases} \dot{\lambda}_D = v_\eta/\rho, \\ \dot{\lambda}_T = -v_\xi/(\rho \cos \lambda_D), \\ \rho = \sqrt{x_i^2 + y_i^2 + z_i^2}, \\ T_g = \rho/v_\xi = -\rho/\dot{\rho}, \end{cases}$$

$$\begin{pmatrix} v_\xi \\ v_\eta \\ v_\zeta \end{pmatrix} = \mathbf{S}_0 \begin{pmatrix} v_x \\ v_y \\ v_z \end{pmatrix} = \mathbf{S}_0 \begin{pmatrix} \dot{x}_i \\ \dot{y}_i \\ \dot{z}_i \end{pmatrix},$$

$$\begin{cases} \dot{x}_i = v_i \cos \theta_i \cos \sigma_i, \\ \dot{y}_i = v_i \sin \theta_i, \\ \dot{z}_i = -v_i \cos \theta_i \sin \sigma_i, \end{cases}$$

$$\mathbf{S}_0 = \begin{bmatrix} \cos \lambda_D \cos \lambda_T & \sin \lambda_D & -\cos \lambda_D \sin \lambda_T \\ -\sin \lambda_D \cos \lambda_T & \cos \lambda_D & \sin \lambda_D \sin \lambda_T \\ \sin \lambda_T & 0 & \cos \lambda_T \end{bmatrix},$$

where v_ξ , v_η and v_ζ are the velocity decomposition described in the LOS Cartesian coordinate system. \mathbf{S}_0 denotes the transform matrix between the target coordinate system and the LOS coordinate system. Then we obtain

$$\begin{cases} \dot{\theta} = -\dot{\lambda}_D / \cos(\lambda_T - \sigma_i), \\ \dot{\sigma} = [\dot{\lambda}_T - \dot{\lambda}_D \tan(\lambda_T - \sigma_i) \sin \lambda_D] / \cos \lambda_D. \end{cases}$$

From (1), we get the lift and side force

$$\begin{cases} Y_i = m v_i \cdot \{\dot{\theta} - \mu/(r^3 v_i) \cdot [x_i \sin \theta_i \cos \sigma_i - (y_i + R_0) \cos \theta_i - z_i \sin \theta_i \sin \sigma_i]\} - P \sin \alpha_{i-1}, \\ Z_i = -m v_i \cos \theta_i \cdot \{\dot{\sigma} + \mu/(r^3 v_i \cos \theta_i) \cdot [x_i \sin \sigma_i + z_i \cos \sigma_i]\} + P \cos \alpha_{i-1} \sin \beta_{i-1}, \end{cases}$$

where r is the radial distance from the center of the earth to the weapon and μ is the gravitational constant while R_0 denotes the mean radius of the Earth. α_{i-1} and β_{i-1} are the angle of attack and sideslip angle of last step. The propulsion P is a constant.

It is assumed that the angle of attack and the sideslip angle are small. Then we can approximately obtain

$$\begin{cases} \alpha_i = Y_i / (C_y^\infty \cdot q \cdot S), \\ \beta_i = Z_i / (C_z^\infty \cdot q \cdot S), \end{cases} \quad (13)$$

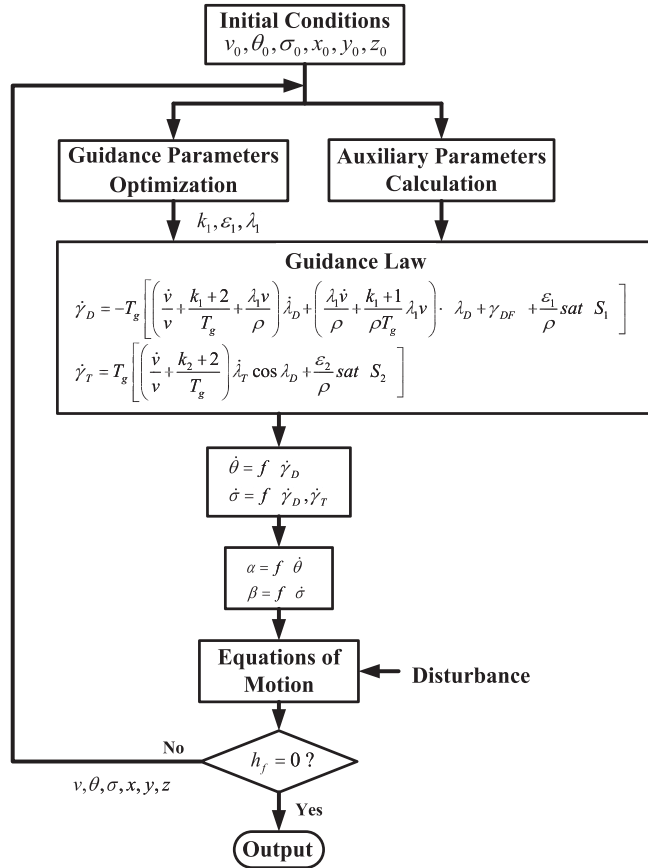


Fig. 2. The circuit of on-line optimization.

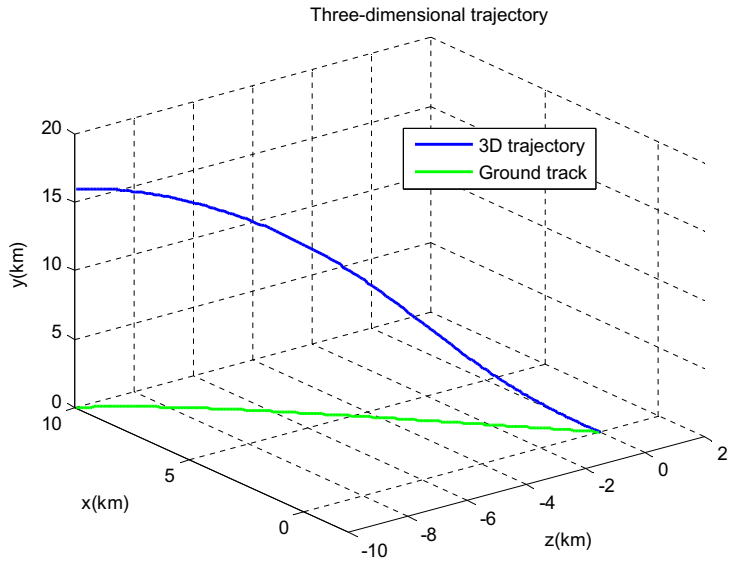


Fig. 3. Three-dimensional trajectory for the ground striking ($\gamma_{DF} = -45^\circ$).

where q is the dynamic pressure. S denotes the reference area. C_y^α and C_z^β are the aerodynamic lift and side force coefficients, respectively. The absolute magnitude of angle of attack and sideslip angle should be limited during the whole striking course by their maximum values α_{\max} and β_{\max} .

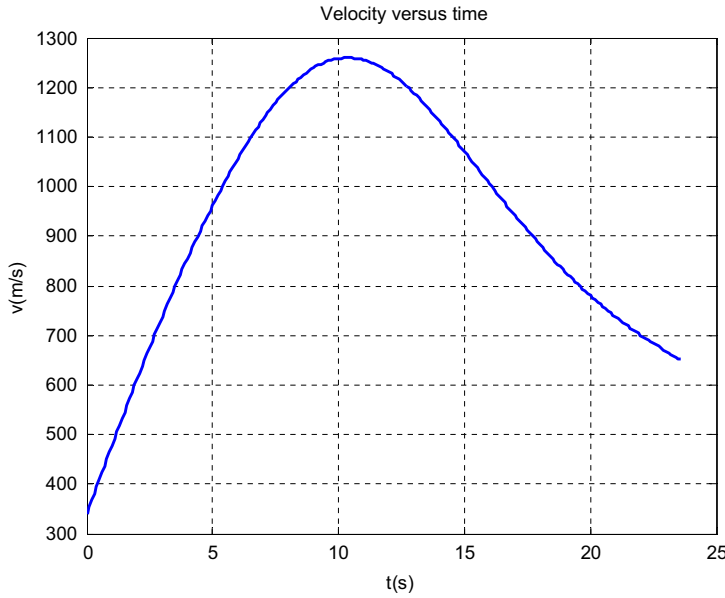


Fig. 4. Velocity profile for the ground striking ($\gamma_{DF} = -45^\circ$).

The drag is approximated by

$$X_i = C_x \cdot q \cdot S,$$

where $C_x = C_{x0} + C_x^z(\alpha_i^2 + \beta_i^2)$. C_{x0} and C_x^z are aerodynamic drag coefficients.

At this moment, the velocity rate is

$$\dot{v}_i = (P \cos \alpha_i \cos \beta_i - X_i)/m - \mu/r^3 \cdot [x_i \cos \theta_i \cos \sigma_i + (y_i + R_0) \sin \theta_i - z_i \cos \theta_i \sin \sigma_i].$$

Then the heating rate constraint, normal load factor constraint and dynamic pressure constraint can be expressed analytically by expressions of the guidance law parameters, respectively.

$$\begin{cases} \dot{Q}_i = \sqrt{\rho_i} (\nu_{i-1} + \dot{v}_i \cdot h)^3 = f(k_1, \varepsilon_1, \lambda_1) \leq \dot{Q}_{\max}, \\ n_{yi} = \sqrt{Y_i^2 + Z_i^2} \cdot \cos \alpha_i + X_i \cdot \sin \alpha_i = f(k_1, \varepsilon_1, \lambda_1) \leq n_{y\max}, \\ q_i = 0.5 \rho_i (\nu_{i-1} + \dot{v}_i \cdot h)^2 = f(k_1, \varepsilon_1, \lambda_1) \leq q_{\max}, \end{cases} \quad (14)$$

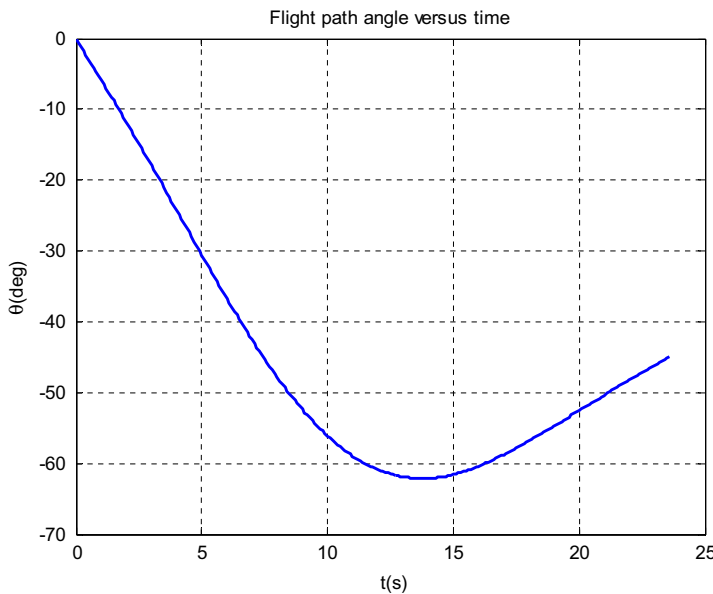


Fig. 5. Flight path angle profile for the ground striking ($\gamma_{DF} = -45^\circ$).

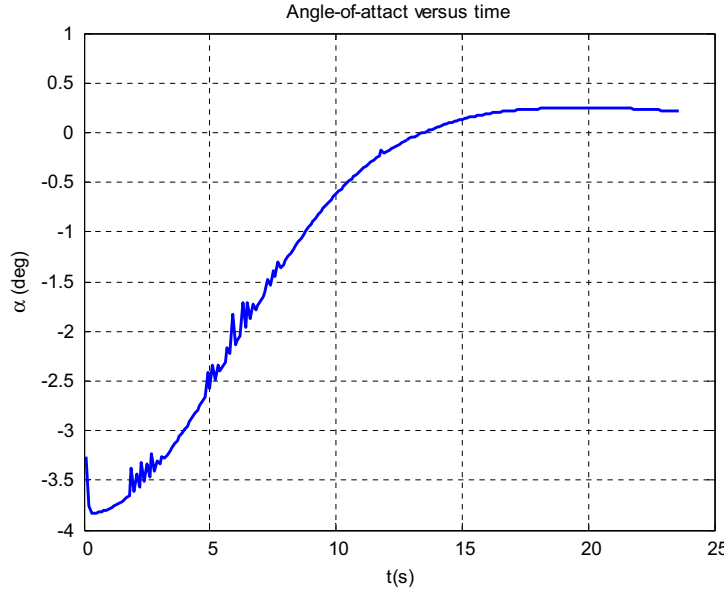


Fig. 6. Angle of attack profile for the ground striking ($\gamma_{DF} = -45^\circ$).

where v_{i-1} is the velocity of last step. \dot{Q}_{\max} , $n_{y\max}$ and q_{\max} are the maximum allowable values of heating rate, normal load factor and dynamic pressure, respectively. Besides, the design variables, i.e. the real-time guidance law parameters, should lie in their upper and lower bounds.

$$0.01 \leq k_1 \leq 2, \quad 0.01 \leq \varepsilon_1 \leq 2, \quad 0.1 \leq \lambda_1 \leq 2.$$

Here we only consider three parameters and choose Δ_1 as the standard constant because of its negligible impact on the guidance performance.

Based on above procession, our crucial target is to find out a series of optimal guidance law parameters which not only satisfy the specified inequality constraints as shown in (13) and (14), but also minimize the performance index in every step. In addition, the design variables should not exceed the upper and lower bounds.

The flow chart of on-line optimization is shown in Fig. 2.

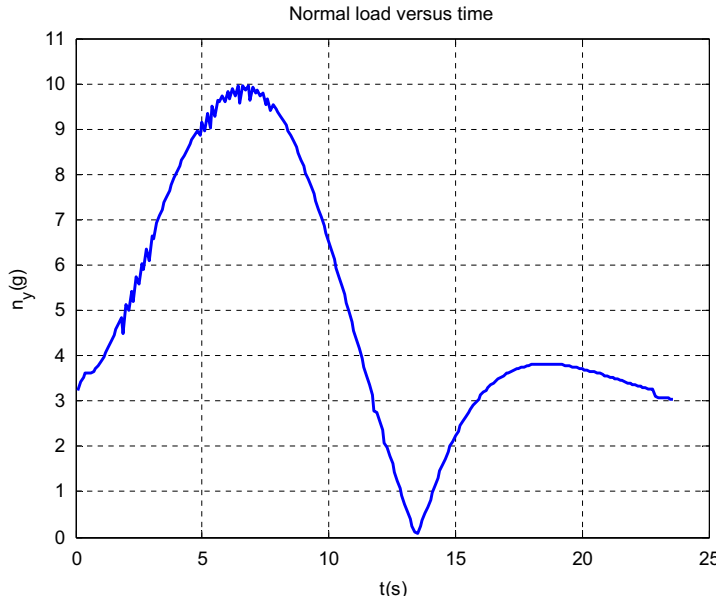


Fig. 7. Normal load factor profile for the ground striking ($\gamma_{DF} = -45^\circ$).

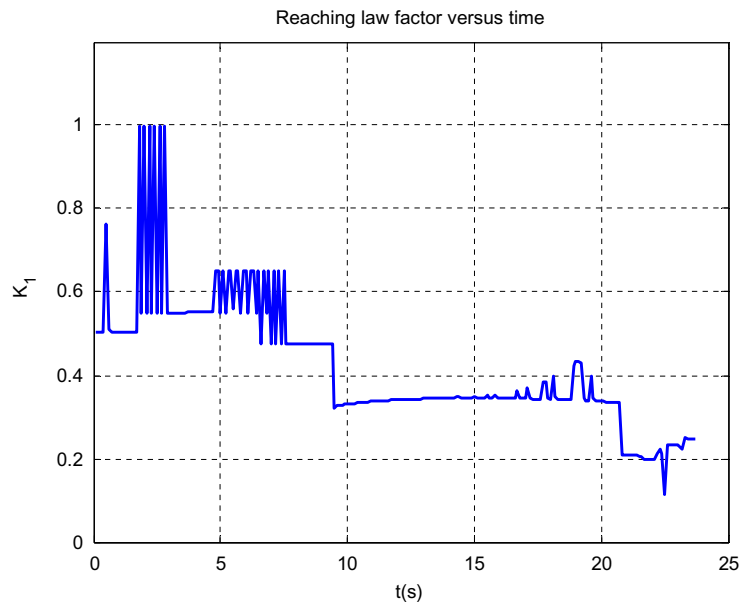


Fig. 8. The optimal history of k_1 for the guidance law ($\gamma_{DF} = -45^\circ$).

6. Simulation studies

The desired impact angle is chosen as $\gamma_{DF} = -45^\circ$ and $\gamma_{DF} = -90^\circ$, respectively, to investigate the properties of the SQP method for the guidance law optimization. The maximum allowable values of these inequality constraints are set at $\alpha_{\max} = 6^\circ$, $\beta_{\max} = 6^\circ$, $\dot{Q}_{\max} = 1,400,000 \text{ kW/m}^2$, $n_{y\max} = 12 \text{ g}$ and $q_{\max} = 350,000 \text{ N/m}^2$. The initial conditions are given in Table 1. This simulation task is carried on a PC with 2G memory and Intel(R) Core(TM) 2 Duo CPU. The version of MATLAB is R2012a.

6.1. Desired impact angle $\gamma_{DF} = -45^\circ$

The simulation results are presented by Figs. 3–10 and Table 6.

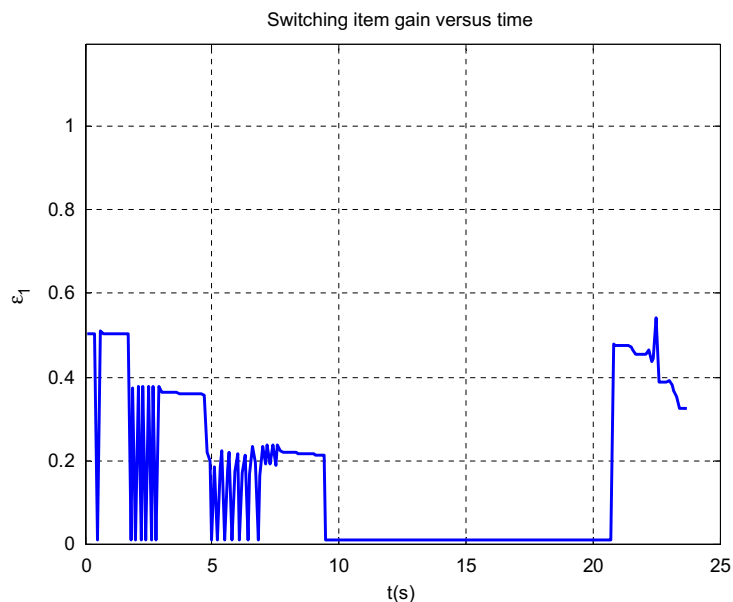


Fig. 9. The optimal history of z_1 for the guidance law ($\gamma_{DF} = -45^\circ$).

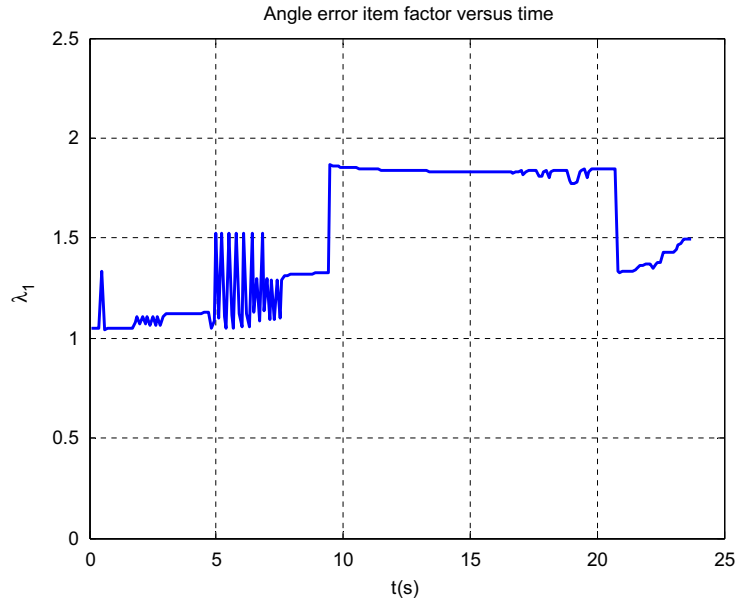


Fig. 10. The optimal history of λ_1 for the guidance law ($\gamma_{DF} = -45^\circ$).

Table 6

Simulation results for ground striking ($\gamma_{DF} = -45^\circ$).

CEP (m)	θ_f ($^\circ$)	α_f ($^\circ$)	v_f (m/s)	J
1.5639	-44.8619	0.2287	651.7479	671.9715

6.2. Desired impact angle $\gamma_{DF} = -90^\circ$

The simulation results are presented by Figs. 11–18 and Table 7.

Figs. 3 and 11 present the three-dimensional striking trajectories and their ground tracks. Figs. 4 and 12 show the time-histories of velocity. Figs. 5 and 13 depict the flight path angle curves from the initial value to the desired impact angle. Figs.

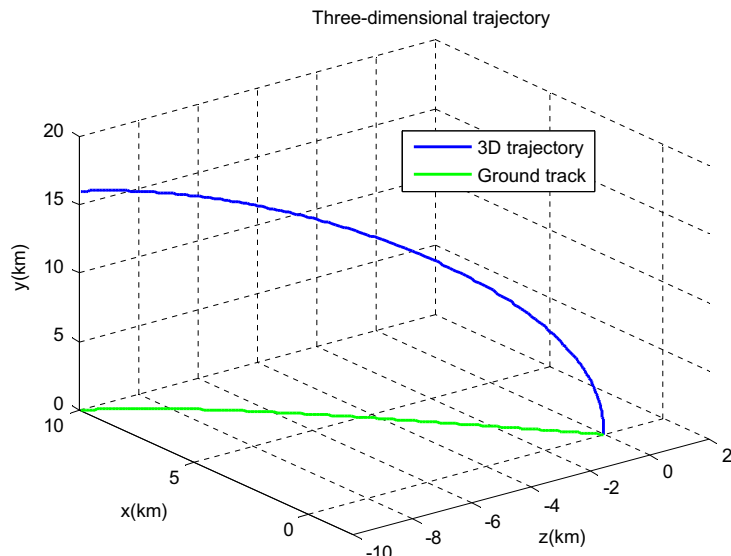


Fig. 11. Three-dimensional trajectory for the ground striking ($\gamma_{DF} = -90^\circ$).

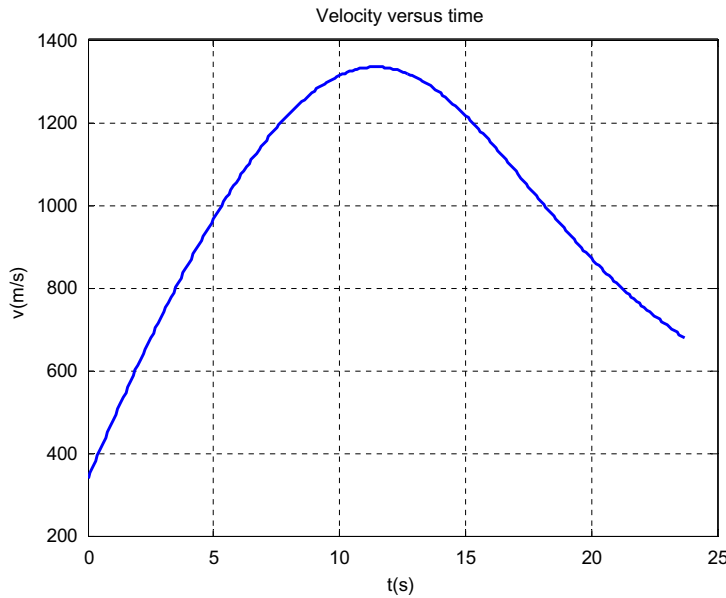


Fig. 12. Velocity profile for the ground striking ($\gamma_{DF} = -90^\circ$).

6 and 14 represent the angle of attack histories and the corresponding normal load factor profiles are shown by Figs. 7 and 15, respectively. By observing Fig. 14 with a desired impact angle of -90° , the values of angle of attack remain negative through the whole striking course to make the trajectory more precipitous, so that the flight path angle can be reduced quickly. However, in the case of -45° desired impact angle, as can be seen from Fig. 6, the magnitude of angle of attack maintains negative during most part of the flying course and then turns to positive to meet the requirement of the desired impact angle. Besides, with the selecting of the optimal guidance law parameters, small daps of the angle of attack emerge during the initial stage of the striking, which can also be observed from the history of normal load factor shown in Figs. 7 and 15. Figs. 8–10 and 16–18 show the optimal profiles of guidance parameters based on the SQP algorithm.

Simulation results for ground striking are given in Tables 6 and 7. By these results, we can find that the SQP method for on-line optimization design of guidance law with multiple constraints is well estimated. Furthermore, when the step size is chosen as 0.5 s, the whole optimization process only costs less than 5 s, while the off-line optimization by genetic algorithm

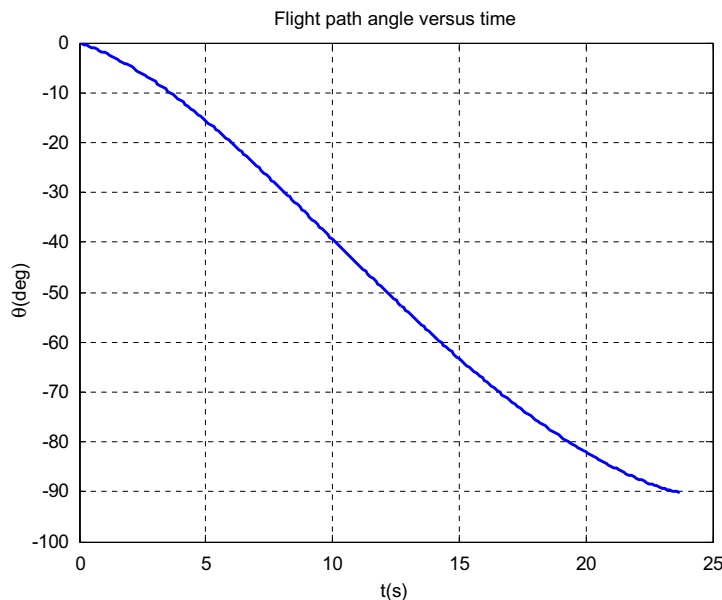


Fig. 13. Flight path angle profile for the ground striking ($\gamma_{DF} = -90^\circ$).

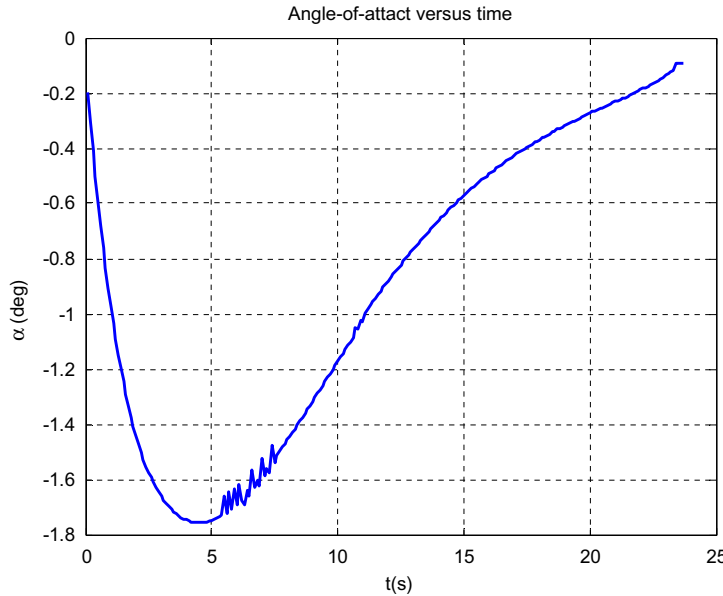


Fig. 14. Angle of attack profile for the ground striking ($\gamma_{DF} = -90^\circ$).

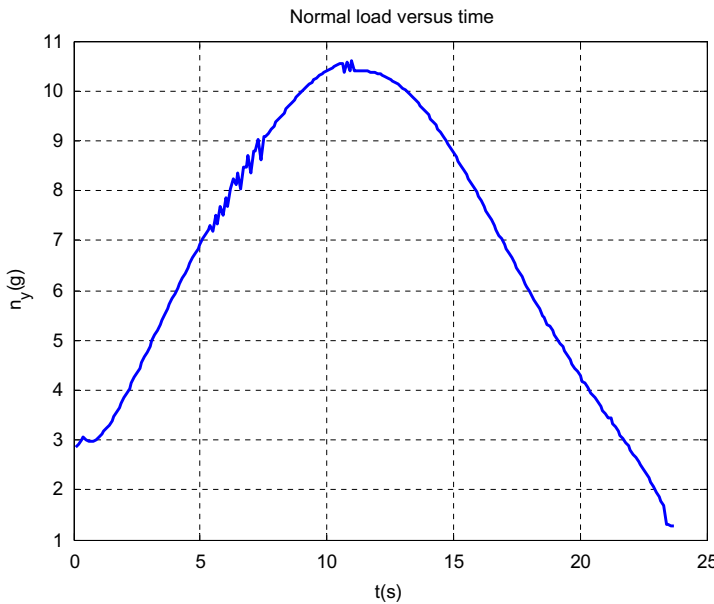


Fig. 15. Normal load factor profile for the ground striking ($\gamma_{DF} = -90^\circ$).

discussed in Hu et al. [33] cost about 20 min. So the optimization strategy proposed in this paper satisfies the requirement of real-time optimization and on-line application.

6.3. Simulation results for different impact angles

An optimization procedure of SMC-based terminal guidance law for impact angle constrained engagement with stationary target is proposed and two cases are studies to illustrate the feasibility of this method. However, it is still not enough to demonstrate and address the performance of this new approach. In this subsection, the magnitude of impact angle is assumed to range from 0 to -90° , and the corresponding miss-distances, impact angles, terminal velocities and angles of attack are reported in Table 8.

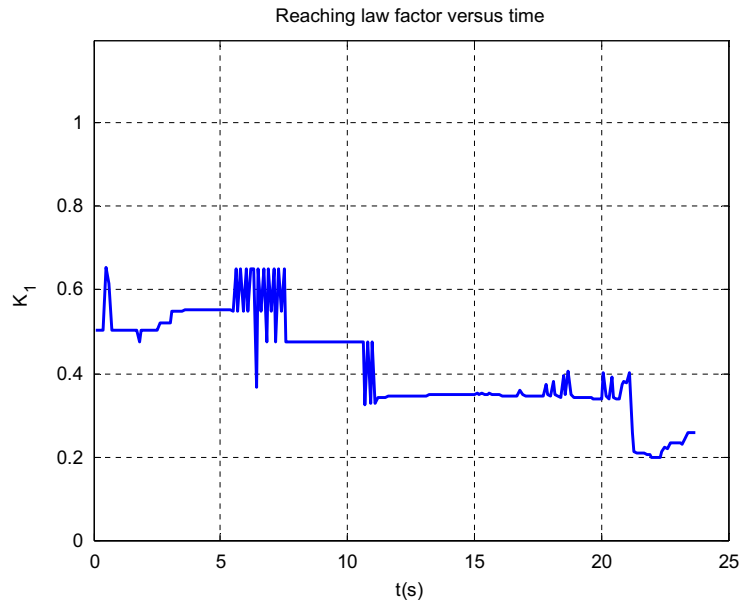


Fig. 16. The optimal history of k_1 for the guidance law ($\gamma_{DF} = -90^\circ$).

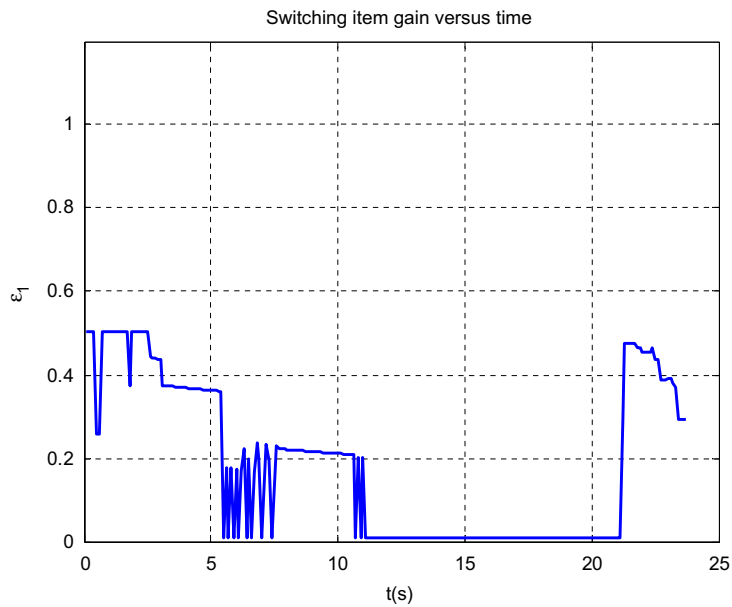


Fig. 17. The optimal history of ε_1 for the guidance law ($\gamma_{DF} = -90^\circ$).

As can be seen from Table 8, the air-to-ground weapon can achieve nearly every desired impact angle ranging from 0 to -90° with high performance after using the sliding mode terminal guidance law and on-line optimization procedure. Both the miss-distances and the terminal angles of attack are small, and the values of terminal heading angle are almost the same as each desired impact angle. Furthermore, the optimal solutions of guidance parameters under each case can be obtained within several seconds based on SQP method.

6.4. Simulation results under initial errors

The air-to-ground guided weapons are usually carried by airplane or even larger transporter to specified position and launched to carry out the striking. However, the accurate toss condition is difficult to reach because of unknown distur-

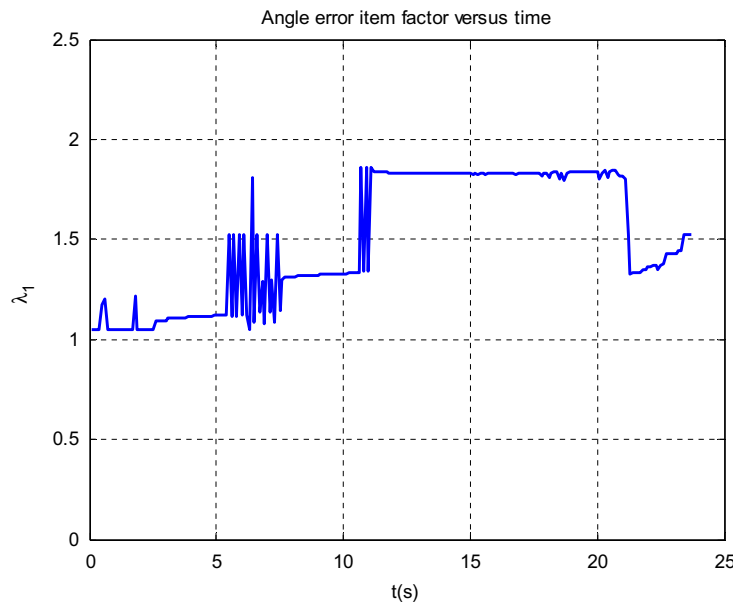


Fig. 18. The optimal history of λ_1 for the guidance law ($\gamma_{DF} = -90^\circ$).

Table 7

Simulation results for ground striking ($\gamma_{DF} = -90^\circ$).

CEP (m)	θ_f ($^\circ$)	α_f ($^\circ$)	v_f (m/s)	J
0.0718	-90.1115	-0.0912	679.1426	664.5976

Table 8

Simulation results for different desired impact angles.

λ_{DF} ($^\circ$)	CEP (m)	θ_f ($^\circ$)	α_f ($^\circ$)	v_f (m/s)
0	2.8187	-0.6613	0.6185	603.0048
-15	2.5522	-14.5442	0.5148	618.9391
-30	2.1803	-29.6635	0.3802	635.8122
-45	1.5639	-44.8619	0.2287	651.7479
-60	1.1970	-59.9764	0.0722	664.8032
-75	1.0399	-75.0553	-0.0701	674.2781
-80	0.6916	-80.0542	-0.1022	675.5686
-85	0.5911	-85.1164	-0.1513	677.7938
-90	0.0718	-90.1115	-0.0912	679.1426

Table 9

Simulation results under initial deviations ($\gamma_{DF} = -90^\circ$).

Initial deviations		CEP (m)	θ_f ($^\circ$)	α_f ($^\circ$)	v_f (m/s)
Initial height h_0	+5%	0.1628	-90.1144	-0.1580	677.9521
	-5%	0.1940	-90.1393	-0.1894	676.4697
Launching range ρ_0	+5%	0.1834	-90.1234	-0.1769	677.3472
	-5%	0.2065	-89.9281	-0.1688	681.0739
Initial velocity v_0	+5%	0.1789	-90.1237	-0.1733	677.3064
	-5%	0.2176	-89.9360	-0.1718	680.8195
Initial heading angle θ_0	+5°	0.2033	-89.9353	-0.1630	681.2305
	-5°	0.1928	-90.1193	-0.1837	677.2561
Initial deflection angle σ_0	+5°	0.0591	-90.1161	-0.1898	679.3136
	-5°	0.0589	-90.1157	-0.1901	679.3184

bances such as navigation errors, atmospheric disturbances and wind interference. A guidance law with strong robustness should be insensitive to these uncertain factors. In order to validate the robustness of the terminal guidance law and its opti-

mization approach, the effect of initial condition deviation on guidance performance is studied and the simulation results are reported in Table 9. The desired impact angle is chosen as $\gamma_{DF} = -90^\circ$.

According to the numerical simulation results, the proposed optimization design of the SMC-based guidance law for stationary target offers good robustness and becomes insensitive to uncertainties. The miss-distances, impact angles and terminal angles of attack under different initial deviations approximate to the results of ideal condition without any disturbances.

7. Conclusions

According to the fact that many kinds of air-to-ground guided weapons are hoped not only to get a minimum miss-distance but also to achieve a desired impact angle to acquire better kill effect, a terminal guidance law based on the SMC methodology was designed to achieve this goal. This paper studies the on-line optimization of the terminal guidance law using SQP algorithm and obtains the optimal history of the guidance parameters corresponding to specified constraints and performance index.

First, the weapon-target engagement model was divided into two separate planes (i.e., the diving plane and the turning plane) and the equations of the striking situation were derived. Then a terminal guidance law was designed using SMC theory to null the miss-distance and achieve a desired impact angle, simultaneously. The chattering of SMC guidance was reduced by the boundary layer approach and formed the Quasi-SMC guidance law. The influence of the four guidance parameters on the guidance performance was discussed as well. Based on the consideration of the real-time requirement and the complex environment of condensed atmosphere, the optimization model of the guidance law was established to satisfy specified constraints (i.e., heating rate, normal load factor, and dynamic pressure) and minimize the performance index, which represents the fuel expenditure and velocity lost. Finally, this optimization model was solved by SQP algorithm and its feasibility was demonstrated through simulation studies under different scenarios.

The new approach discussed in this paper serves as a useful and efficient mean on the design and optimization of the guidance system for the anti-tank or anti-ship missiles, the precision guided penetrating bombs and some other guided weapons. According to the simulation results, the proposed on-line optimization design of the sliding mode guidance law not only satisfies the specified constraints, but also minimizes the fuel cost during the whole striking course. What is more important is the optimization process can be completed in a few seconds, which is suitable for on-board application of ground striking. Future work in this area could focus on developing new optimization strategies for the design of guidance laws. The proposed new approach could be extended to solve the optimization problems of new guidance laws under different engagement scenarios, for example, the high order sliding mode guidance laws for air-to-ground guided weapons, the adaptive sliding mode guidance laws for air-to-air missiles, and the fuzzy sliding mode guidance laws for anti-ship missiles, and so on.

Acknowledgments

Thanks for the supports of the National Science and Technology Support Program of China under Grant No. 2011BAK16B03. Technical discussions with Dr. Yongqing Tian are gratefully acknowledged.

Appendix A. Supplementary data

Supplementary data associated with this article can be found, in the online version, at <http://dx.doi.org/10.1016/j.apm.2013.02.030>.

References

- [1] M. Kim, K.V. Grider, Terminal guidance for impact attitude angle constrained flight trajectories, *IEEE Trans. Aerosp. Electron. Syst.* 9 (6) (1973) 852–859.
- [2] T.L. Song, S.J. Shin, H. Cho, Impact angle control for planar engagements, *IEEE Trans. Aerosp. Electron. Syst.* 35 (4) (1999) 1439–1444.
- [3] C.K. Ryoo, H. Cho, M.J. Tahk, Closed-form solutions of optimal guidance with terminal impact angle constraint, in: Proceedings of the IEEE Conference on Control Applications, 2003, pp. 504–509.
- [4] Y. Lee, C.K. Ryoo, E. Kim, Optimal guidance with constraints on impact angle and terminal acceleration, in: AIAA Guidance, Navigation, and Control Conference, Austin, TX, Aug. 2003.
- [5] C.K. Ryoo, H. Cho, M.J. Tahk, Optimal guidance laws with terminal impact angle constraint, *AIAA J. Guidance Control Dyn.* 28 (4) (2005) 724–732.
- [6] C.K. Ryoo, H. Cho, M.J. Tahk, Time-to-go weighted optimal guidance with impact angle constraints, *IEEE Trans. Control Syst. Technol.* 14 (3) (2006) 483–492.
- [7] J.I. Lee, B.M. Min, M.J. Tank, Suboptimal guidance laws with terminal jerk constraint, in: 2007 International Conference on Control, Automation and Systems (ICCAS), 2007, pp. 1399–1403.
- [8] S. Subchan, An indirect method for the minimum altitude of air-to-surface missile, in: 2008 Third IEEE Conference on Industrial Electronics and Applications (ICIEA), 2008, pp. 126–131.
- [9] P.B. Ma, Y.A. Zhang, J. Ji, X.J. Zhang, Three-dimensional guidance law with terminal impact angle constraint, in: Proceedings of the IEEE Conference on Mechatronics and Automation, 2009, pp. 4162–4166.
- [10] Y. Kim, J. Kim, M. Park, Guidance and control system design for impact angle control of guided bombs, in: International Conference on Control, Automation and Systems, KINTEX, Gyeonggi-do, Korea, 2010, pp. 2138–2143.

- [11] H.B. Oza, R. Padhi, A nonlinear suboptimal guidance law with 3D impact angle constraints for ground targets, in: AIAA Guidance, Navigation, and Control Conference, Toronto, Ontario, Canada, Aug. 2010, pp. 1–25.
- [12] H.B. Oza, R. Padhi, Impact-angle-constrained suboptimal model predictive static programming guidance of air-to-ground missiles, *AIAA J. Guidance Control Dyn.* 35 (1) (2012) 153–164.
- [13] Q. Xing, W.C. Chen, Segmented optimal guidance with constraints on terminal angle of attack and impact angle, in: 2012 50th AIAA Aerospace Sciences Meeting including the New Horizons Forum and Aerospace Exposition, Nashville, TN, Jan. 2012, pp. 1–10.
- [14] Y.I. Lee, S.H. Kim, J.I. Lee, Analytic solutions of generalized impact-angle-control guidance law for first-order lag system, *AIAA J. Guidance Control Dyn.*, 2012, pp. 1–17 (Published online).
- [15] Y.I. Lee, S.H. Kim, M.J. Tahk, Analytic solutions of optimal angularly constrained guidance for first-order lag system, in: Proceedings of the Institution of Mechanical Engineers, Part G: Journal of Aerospace Engineering, 2012, pp. 1–11 (Published online).
- [16] Y.I. Lee, S.H. Kim, M.J. Tahk, Optimality of linear time-varying guidance for impact angle control, *IEEE Trans. Aerosp. Electron. Syst.* 48 (4) (2012) 2802–2817.
- [17] B.S. Kim, J.G. Lee, H.S. Han, Biased PNG law for impact with angular constraint, *IEEE Trans. Aerosp. Electron. Syst.* 34 (1) (1998) 277–288.
- [18] J.M. Song, T.Q. Zhang, Passive homing missile's variable structure proportional navigation with terminal angular constraint, *Chin. J. Aeronaut.* 14 (2) (2001) 83–87.
- [19] S.K. Jeong, S.J. Cho, E.G. Kim, Angle constraint biased PNG, in: 2004 5th Asian Control Conference, 2004, pp. 1849–1854.
- [20] Z.D. Hu, H. Cai, An adaptive proportional guidance law against ground stationary target, in: 2008 Second International Symposium on Systems and Control in Aerospace and Astronautics (ISSCAA), 2008, pp. 1–5.
- [21] A. Ratnoot, D. Ghose, Impact angle constrained interception of stationary targets, *AIAA J. Guidance Control Dyn.* 31 (6) (2008) 1817–1822.
- [22] A. Ratnoot, D. Ghose, Satisfying terminal angular constraint using proportional navigation, in: AIAA Guidance, Navigation, and Control Conference, Chicago, IL, Aug. 2009.
- [23] A. Ratnoot, D. Ghose, Impact angle constrained guidance against nonstationary nonmaneuvering targets, *AIAA J. Guidance Control Dyn.* 33 (1) (2010) 269–275.
- [24] K.S. Erer, O. Merttopcuoglu, Indirect control of impact angle against stationary targets using biased PPN, in: AIAA Guidance, Navigation, and Control Conference, Toronto, Ontario, Canada, Aug. 2010, pp. 1–7.
- [25] K.S. Erer, O. Merttopcuoglu, Indirect impact-angle-control against stationary targets using biased pure proportional navigation, *AIAA J. Guidance Control Dyn.* 35 (2) (2012) 700–703.
- [26] G. Akhil, D. Ghose, Biased PN based impact angle constrained guidance using a nonlinear engagement model, 2012 American Control Conference (ACC), 2012, pp. 950–955.
- [27] S.D. Brierley, R. Longchamp, Application of sliding-mode control to air-to-air interception problem, *IEEE Trans. Aerosp. Electron. Syst.* 26 (2) (1990) 306–325.
- [28] B.S. Kim, J.G. Lee, H.S. Han, C.G. Park, Homing guidance with terminal angular constraint against nonmaneuvering and maneuvering targets, in: AIAA Guidance, Navigation, and Control Conference, New Orleans, LA, Aug. 1997, pp. 189–199.
- [29] D. Zhou, C.D. Mu, Q. Ling, W.L. Xu, Optimal sliding-mode guidance of a homing-missile, in: Proceedings of the 38th Conference on Decision and Control, vol. 5, 1999, pp. 5131–5136.
- [30] D. Zhou, C.D. Mu, W.L. Xu, Adaptive sliding-mode guidance of a homing missile, *AIAA J. Guidance Control Dyn.* 22 (4) (1999) 589–594.
- [31] Q.J. Xu, J.D. Yu, J.Y. Yu, X.Z. Yang, Integrated guidance/autopilot design for missiles with impact angle constraints, in: 2006 IEEE International Conference on Information Acquisition, 2006, pp. 75–79.
- [32] W.M. Sun, Z.Q. Zheng, 3D variable structure guidance law based on adaptive model-following control with impact angular constraints, in: 2007 Chinese Control Conference (CCC), 2007, pp. 61–66.
- [33] Z.D. Hu, H.Z. Zhang, H. Cai, Variable structure guidance law of re-entry maneuvering warhead with terminal angular constraint, *Syst. Eng. Electron.* 31 (2) (2009) 393–398 (in Chinese).
- [34] P. Wu, M. Yang, Integrated guidance and control design for missile with terminal impact angle constraint based on sliding mode control, *J. Syst. Eng. Electron.* 21 (4) (2010) 623–628.
- [35] W.J. Gu, Z.E. Fan, X.J. Zhang, Design of variable structure guidance law with constraints on impact angle for anti-ship missile, in: International Conference on Computer Design and Applications, vol. 4, 2010, pp. V480–V484.
- [36] J.G. Guo, J. Zhou, Integrated guidance and control of homing missile with impact angular constraint, in: 2010 International Conference on Measuring Technology and Mechatronics Automation (ICMTMA), 2010, pp. 480–483.
- [37] J.G. Guo, J. Zhou, Integrated guidance-control system design based on H8 control, in: 2010 International Conference on Electrical and Control Engineering (ICECE), 2010, pp. 1204–1207.
- [38] Y.X. Zhang, G.L. Jiao, M.W. Sun, Finite time convergent sliding-mode guidance law with impact angle constraint, in: Proceedings of the 30th Chinese Control Conference, Yantai, China, 2011, pp. 2597–2601.
- [39] Z.D. Hu, X.M. Tang, Y.P. Wang, A 3-dimensional robust guidance law with impact angle constraint, in: Proceedings of the Chinese Control and Decision Conference, Mianyang, China, 2011, pp. 999–1006.
- [40] N. Harl, S.N. Balakrishnan, Impact time and angle guidance with sliding mode control, *IEEE Trans. Control Syst. Technol.* 20 (6) (2012) 1436–1449.
- [41] S.R. Kumar, S. Rao, D. Ghose, Non-singular terminal sliding mode guidance and control with terminal angle constraints for non-maneuvering targets, in: 2012 12th International Workshop on Variable Structure Systems (VSS), 2012, pp. 291–296.
- [42] S.R. Kumar, S. Rao, D. Ghose, Sliding mode guidance and control for all aspect interceptors with terminal angle constraints, *AIAA J. Guidance Control Dyn.* 35 (4) (2012) 1230–1246.
- [43] I.R. Manchester, A.V. Savkin, Circular navigation guidance law for precision missile/target engagements, in: 2002 41st IEEE Conference on Decision and Control, 2002, pp. 1287–1292.
- [44] A. Ratnoot, D. Ghose, SDRE based guidance law for impact angle constrained trajectories, in: AIAA Guidance, Navigation and Control Conference and Exhibit, Hilton Head, South Carolina, Aug. 2007, pp. 1–16.
- [45] A. Ratnoot, D. Ghose, State-dependent Riccati-equation-based guidance law for impact-angle-constrained trajectories, *AIAA J. Guidance Control Dyn.* 32 (1) (2009) 320–325.
- [46] R. Bardhan, D. Ghose, Intercepting maneuvering target with specified impact angle by modified SDRE technique, 2012 American Control Conference (ACC), 2012, pp. 4613–4618.
- [47] J. Yun, C.K. Ryoo, Integrated guidance and control law with impact angle constraint, in: 2011 11th International Conference on Control, Automation and Systems (ICCAS), 2011, pp. 1239–1243.
- [48] A. Dhabale, D. Ghose, Impact angle constraint guidance law using cubic splines for intercepting stationary targets, in: AIAA Guidance, Navigation, and Control Conference, Minneapolis, Minnesota, Aug. 2012, pp. 1–12.
- [49] J.P. Zhang, Y.L. Cao, X.N. Song, M.L. Zhang, G.Z. Shen, 3D guidance for vertical impact on non-stationary targets, in: 2012 IEEE International Conference on Automation and Logistics (ICAL), 2012, pp. 272–276.
- [50] Y.A. Zhang, Y.G. Zhang, L. Heng, Impact time and impact angle control based on CCC path planning, in: 2012 31st Chinese Control Conference (CCC), 2012, pp. 4300–4305.
- [51] C.H. Lee, T.H. Kim, M.J. Tahk, I.H. Whang, Polynomial guidance laws considering terminal impact angle and acceleration constraints, *IEEE Trans. Aerosp. Electron. Syst.* 49 (1) (2013) 74–92.
- [52] H.Y. Zhao, Vehicle Reentry Dynamics and Guidance, National University of Defence Technology Publishing Press, Changsha, China, 1997, pp. 214–232.
- [53] S.C. Chung, C.L. Lin, A transformed lure problem for sliding mode control and chattering reduction, *IEEE Trans. Autom. Control* 44 (3) (1999) 563–568.

- [54] O.V. Stryk, R. Bulirsch, Direct and indirect methods for trajectory optimization, *Ann. Oper. Res.* 37 (1–4) (1992) 357–373.
- [55] F. Tao, D. Zhao, Y.F. Hu, Z.D. Zhou, Resource service composition and its optimal-selection based on particle swarm optimization in manufacturing grid system, *IEEE Trans. Ind. Inf.* 4 (4) (2008) 315–327.
- [56] F. Tao, D. Zhao, Y.F. Hu, Z.D. Zhou, Correlation-aware resource service composition and optimal-selection in manufacturing grid, *Eur. J. Oper. Res.* 201 (1) (2010) 129–143.
- [57] F. Tao, D. Zhao, L. Zhang, Resource service optimal-selection based on intuitionistic fuzzy set and non-functionality QoS in manufacturing grid system, *Knowl. Inf. Syst.* 25 (1) (2010) 185–208.
- [58] F. Tao, K. Qiao, L. Zhang, Z. Li, A.Y.C. Nee, GA-BHTR: an improved genetic algorithm for partner selection in virtual manufacturing, *Int. J. Prod. Res.* 50 (8) (2012) 2079–2100.
- [59] F. Tao, Y.J. Lai, L. Xu, L. Zhang, FC-PACO-RM: a parallel method for service composition optimal-selection in cloud manufacturing system, *IEEE Trans. Ind. Inf.*, in press.
- [60] F. Tao, L. Zhang, Y.F. Hu, *Resource Services Management in Manufacturing Grid System*, Wiley, Scrivener Publishing, MA, USA, 2012, ISBN 978-1-118-12231-0.
- [61] P.E. Gill, W. Murray, M.A. Saunders, SNOPT: an SQP algorithm for large-scale constrained optimization, *Soc. Ind. Appl. Math. Rev.* 47 (1) (2005) 99–131.
- [62] P.S. Els, P.E. Uys, J.A. Snyman, M.J. Thoreson, Gradient-based approximation methods applied to the optimal design of vehicle suspension systems using computational models with severe inherent noise, *Math. Comput. Model.* 43 (7–8) (2006) 787–801.
- [63] P.Y. Nie, An SQP approach with line search for a system of nonlinear equations, *Math. Comput. Model.* 43 (3–4) (2006) 368–373.
- [64] D.N. Zhang, Y. Liu, RLV reentry trajectory optimization through hybridization of an improved GA and a SQP Algorithm, in: AIAA Guidance, Navigation, and Control Conference, Portland, Oregon, 2011.
- [65] A. Barclay, P.E. Gill, J.B. Rosen, SQP methods and their application to numerical optimal control, NA 97-3, Department of Mathematics, University of California, San Diego, 1997.